Effects of Screw Configurations on the Grafting of Maleic Anhydride Grafted Low-Density Polyethylene in Reactive Extrusion

Hui Fang, Xiuqing Ma, Lianxun Feng, Kuisheng Wang, Bin Cao

Beijing University of Chemical Technology, Beijing 100029, China

Received 28 September 2006; accepted 8 July 2007
DOI 10.1002/app.27158
Published online 7 March 2008 in Wiley InterScience (www.interscience.wiley.com).

ABSTRACT: The effects of screw configurations, that is, the staggering angles and disc widths of the kneading blocks, on grafting reactive extrusion for maleic anhydride grafted low-density polyethylene were investigated in a corotating twin-screw extruder. Samples were collected from three positions along the screw and the die exit. The grafting degree (GD) of the specimens was evaluated by titration. It was found that the kneading block configurations had a significant influence on the grafting reactive extrusion. In addition, another three groups of extrusion experiments were performed to explore the intrinsic relationship between the GD, the degree of fill in the screw channel, the residence time distribution (RTD), and the mixing intensity in various screw configurations. The experimental results indicated that the location of the melting endpoint significantly affected the position at which the reaction began; the degree of fill, RTD, and mixing performance of the screw played important roles in the grafting reaction. The reverse kneading blocks with a narrow disc width, which had a high degree of fill and good mixing capacity, enhanced the increase in GD along the screw during the reactive extrusion. © 2008 Wiley Periodicals, Inc. J Appl Polym Sci 108: 3652–3661, 2008

Key words: graft copolymers; polyethylene (PE); reactive extrusion

INTRODUCTION

The chemical modification of thermoplastics in twin-screw extruders is a widely used approach to tailor the properties of polymers according to their applications. Carrying out the reaction via extrusion has economic advantages, such as a short reaction time and a solvent-free process.[1] Twin-screw extruders as continuous flow reactors for polymers have been playing an important role in producing high-performance materials.

Free-radical grafting of maleic anhydride (MA) onto polyethylene (PE) via reactive extrusion has gained widespread industrial applications and has been studied by numerous authors. Several studies have shown that the reaction pathways depend on the PE molecular structure.[2–5] When peroxide is used as an initiator, crosslinking may occur simultaneously with the grafting reaction.[6–11] Furthermore, the analysis of the reactive extrusion process is very complicated because of the multiple operating variables involved. A number of interdependent factors need to be determined and optimized to maximize the efficiency of the process.[11–16]

Most grafting studies of PE in reactive extrusion focus on the effects of grafting recipes (type and amount of peroxide and MA content) and processing conditions (throughput and temperature) on the reaction progression in the extruder. The aforementioned factors are important in reactive extrusion. However, it has been well known for years that the mixing method strongly influences the grafting process of PE in the extruder. The mixing of the monomer (MA), initiator (peroxide), and polymer melt is very critical in the manufacturing of high-grafting products, and the screw configuration, a core component of an extruder, has a significant impact on the reactive extrusion process.

In this work, the influence of various screw configurations on grafting reactive extrusion was investigated with a corotating twin-screw extruder. To further explore the effects of the degree of fill, residence time distribution (RTD), and mixing performance of screws on grafting reactive extrusion, another three extrusion experiments were performed to evaluate these properties.

EXPERIMENTAL

Materials

Low-density polyethylene [LDPE; LD-100, melt flow index = 2.0 g/10 min (190°C, 2.16 kg)] was supplied by China SINOPEC Beijing Yanshan Chemical Co.

Correspondence to: X. Ma (maxq@mail.buct.edu.cn).
Contract grant sponsor: Committee of China National Natural Science Foundation; contract grant number: 50390090.

Journal of Applied Polymer Science, Vol. 108, 3652–3661 (2008)

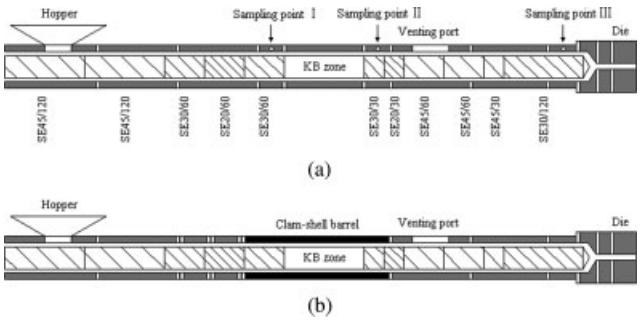

Figure 1 Screw configuration and barrel structure: (a) screw configurations and barrel structure for ExI, ExIII, and ExIV and (b) screw configuration and barrel structure for ExII.

(Beijing, China) Dicumyl peroxide, obtained from Shanghai Chemical Reagent Co. (China Pharmacy Group, Shanghai, China), was recrystallized twice from absolute alcohol before use. MA, xylene, and acetone were provided by Beijing Yili Fine Chemical Co., Ltd. (Beijing, China) Polycarbonate [PC; PC-110, melt flow index = 10 g/10 min (300°C, 1.2 kg)] and acrylonitrile butadiene styrene [ABS; PA-747S, melt flow index = 0.7 g/10 min (200°C, 5 kg)] were purchased from Chi Mei Corp. (Zhenjiang, China)

Screw configurations and barrel

In this study, four groups of extrusion experiments were performed in a laboratory modular Leistritz LSM 30.34 intermeshing, corotating twin-screw extruder (Nuremberg, Germany). The screw diameter was 34 mm, the distance between the two screw axes was 30 mm, and the active barrel length was 870 mm (length/diameter = 25.6). These four groups of extrusion processes were designated ExI, ExII, ExIII, and ExIV. These experiments were designed to evaluate the grafting degree (GD) of maleic anhydride grafted low-density polyethylene (LDPE-*g*-MA) during the reactive extrusion, the degree of fill along the screw channel, the RTD, and the mixing performance of the screw configurations. In each group of experiments, seven screw configurations were investigated. Their differences were only in the kneading block zone (KB zone; Fig. 1). The geometry parameters of the kneading blocks in the KB zone are listed in detail in Table I. The screw configurations are named on the basis of the kneading block used in the KB zone. Screws KB30, KB60, KB90, KB120, and KB150 had kneading blocks with different staggering angles, whereas the kneading discs in screw configurations KB90-2 and KB90-4 were wider than the others. As shown in Figure 1(a), the barrel in ExI, ExIII, and ExIV comprised five modular barrel sections and three online sampling instruments. A clam-shell barrel was used in ExII, as depicted in Figure 1(b), which allowed the quick quenching of the polymer melt along the screw channel. A solidified carcass was used to measure the degree of fill along the screw channel and the polymer melting endpoint.

The online sampling equipment used in this study is illustrated in Figure 2. The circular aperture in the barrel wall allowed the flow of the melt out of the extruder. Through the rotation of the valve, the circular aperture could be switched conveniently. In the process of online sampling, the valve was first turned on, and when enough material was collected, the valve was turned off, and then the collecting pot was pulled out. The sample was removed and quenched for subsequent analysis. Generally, it took 3–5 s to sample about 3 g of the polymer melt; this depended on the flow rate and degree of fill.

Processing

The materials and the processing conditions for each experiment are listed in Table II. In the reactive extrusion, the sampling was performed at distances of 400, 560, 840, and 950 mm (the die exit) from the feeding port. To avoid further reaction, the specimens were dipped into liquid nitrogen immediately after being collected from the extruder. To eliminate the residual monomer, the grafted products were dissolved in xylene under reflux until a clear solution was obtained. These solutions were then precipitated in acetone and filtered to obtain the purified products. In the end, the filter mass was dried in a vacuum oven for 24 h at 110°C.

All of the purified specimens were tested for the GD by neutralization titration. Grafted LDPE (0.2 g) was dissolved in 50 mL of xylene at the boiling tem-

TABLE I
Geometry Parameters of the Kneading Blocks for Each Screw Configuration

Screw code	Staggering angle (°)	Disc width (mm)	Disc number	Block length (mm)	Conveying property
KB30	30	7.5	16	120	Forward
KB60	60	7.5	16	120	Forward
KB90	90	7.5	16	120	Neutral
KB120	120	7.5	16	120	Reversed
KB150	150	7.5	16	120	Reversed
KB90-2	90	15	8	120	Neutral
KB90-4	90	30	4	120	Neutral

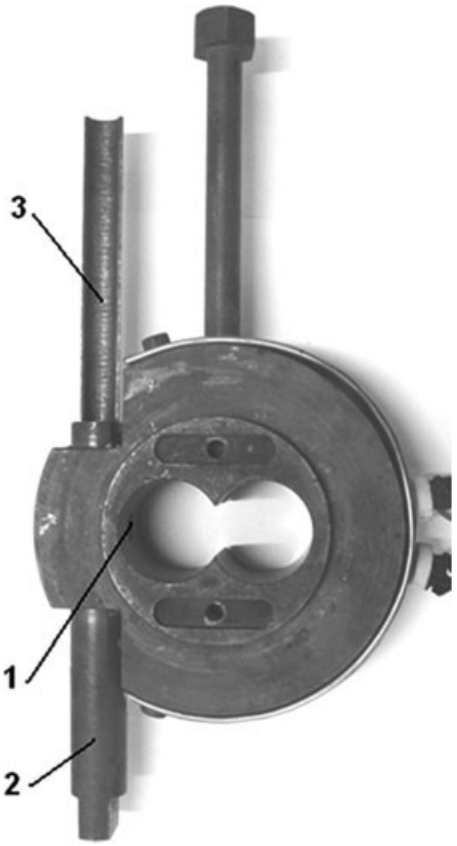

Figure 2 Online sampling equipment: (1) circular aperture, (2) valve, and (3) collecting pot.

perature. When the samples were fully soluble, two to three drops of a colored indicator and excessive KOH–ethanol were added until the solution turned red. Then, HCl–ethanol was added, and the titration was stopped immediately at the visual endpoint when the color changed. GD was calculated with the following equation:

$$\mathrm{GD} = \frac{(N_1V_1 - N_2V_2) \times 98.06 \times 10^{-3}}{2W} \times 100\% \quad (1)$$

where N_1 is the concentration of the KOH–ethanol solution, V_1 is the volume of the added KOH–ethanol solution, N_2 is the concentration of the HCl–ethanol solution, V_2 is the volume of the titrated HCl–ethanol solution, 98.06 is the molecular weight value of MA, and W is the mass of the sample.

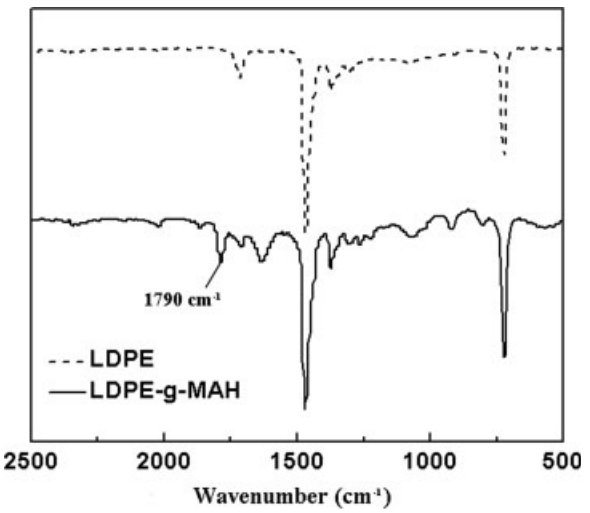

Figure 3 FTIR spectra of LDPE and LDPE-*g*-MA.

In ExII, when the extrusion process was stable, the clam-shell barrel was quenched with cooling water. The carcass was collected after the clam-shell barrels were removed and was further used not only to identify the melting endpoint but also to measure the degree of fill in the kneading blocks.

A pulse stimulus response technique was used to obtain the data for RTD. A blue master batch as a tracer was added to the feeding port after the extrusion reached stable status. The extrudate was collected from the moment right after the feeding of the tracer into the feeding port to the point when all the tracers exited the die. The a^* value (of the $L^*a^*b^*$ color space) was used as the measurement of the tracer concentration in the extrudate.[17,18] To analyze RTD, an $E(t)$ curve was applied, which represents the variation of the concentration of the tracer at the die exit with time. The mean residence time ($\bar{t}$) and the RTD spread around the mean (σ^2; also called the variance) were

TABLE II
Material and Processing Conditions in the Experiments

Experiment group	ExI	ExII	ExIII	ExIV
Subject	Reactive extrusion	Degree of fill	RTD	Mixing ability
Materials	LDPE + MA + DCP (100/3/0.1)	LDPE	LDPE + blue master batch	ABS + PC (80/20)
Feeding rate (kg/h)	7.2	7.2	7.2	7.2
Screw rotation speed (rpm)	30	30	30	30
Temperature of the barrel (°C)	150/160/160/160/160	150/160/160/160/160	150/160/160/160/160	220/230/230/230/230
Temperature of the die (°C)	150	150	150	220

TABLE III
GDs of All Samples for Various Screw Configurations (Average of Three to Five Measurements)

Screw code	GD [wt % (standard deviation)]				Increment in the GDs between the first and second sampling points (wt %)
	Sampling point I	Sampling point II	Sampling point III	Die exit	
KB30	0.090 (0.005)	0.190 (0.009)	0.342 (0.015)	0.682 (0.030)	0.100
KB60	0.074 (0.006)	0.177 (0.008)	0.320 (0.016)	0.639 (0.026)	0.103
KB90	0.093 (0.004)	0.199 (0.010)	0.349 (0.017)	0.720 (0.029)	0.106
KB120	0.115 (0.005)	0.228 (0.011)	0.409 (0.017)	0.760 (0.032)	0.113
KB150	0.098 (0.007)	0.204 (0.010)	0.373 (0.016)	0.721 (0.033)	0.106
KB90-2	0.076 (0.006)	0.175 (0.009)	0.279 (0.014)	0.602 (0.029)	0.099
KB90-4	0.022 (0.004)	0.101 (0.007)	0.230 (0.012)	0.431 (0.026)	0.079

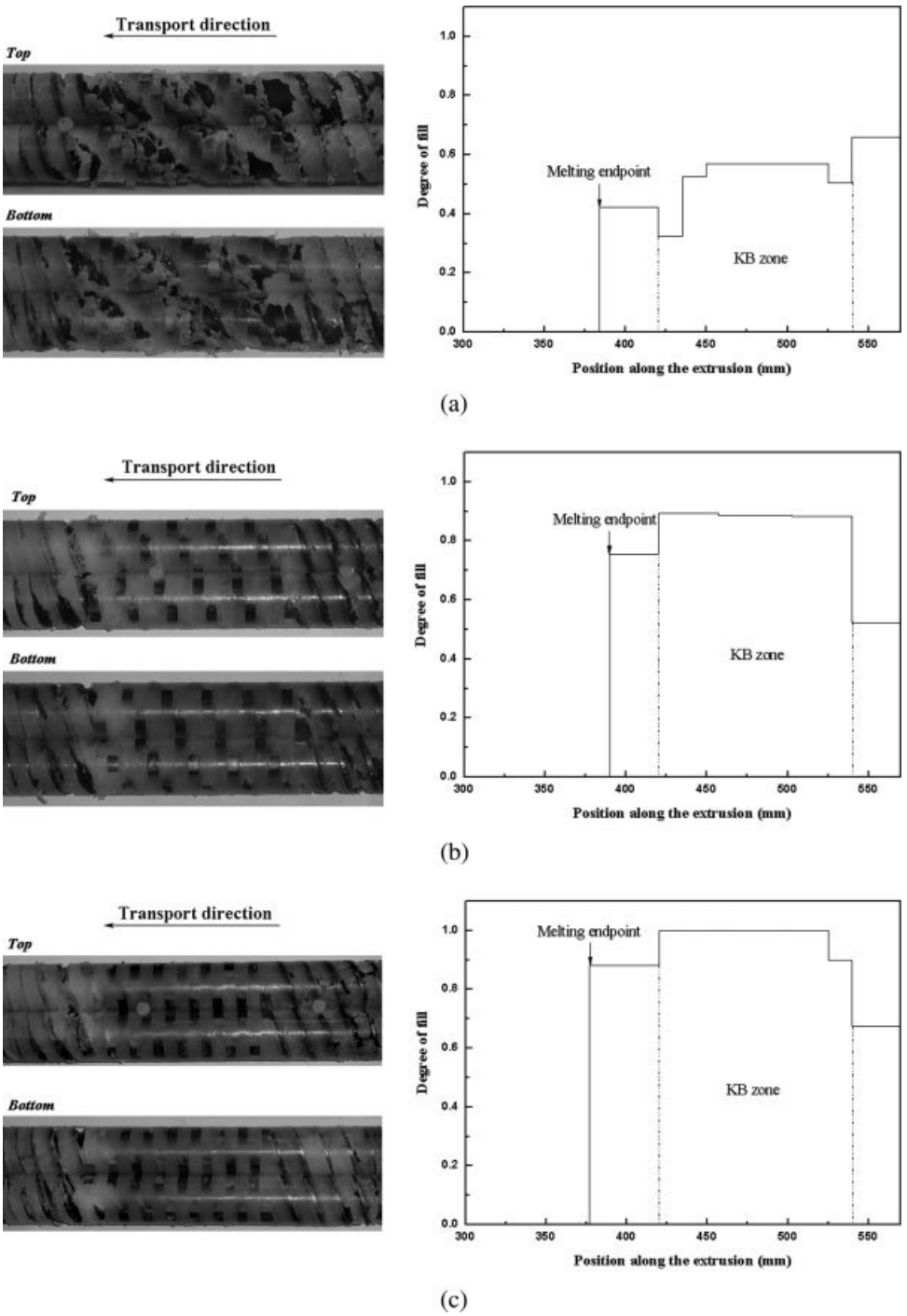

Figure 4 Melting endpoint and degree of fill around the kneading blocks for the screw configurations with various staggering angles: (a) KB30, (b) KB60, (c) KB90, (d) KB120, and (e) KB150.

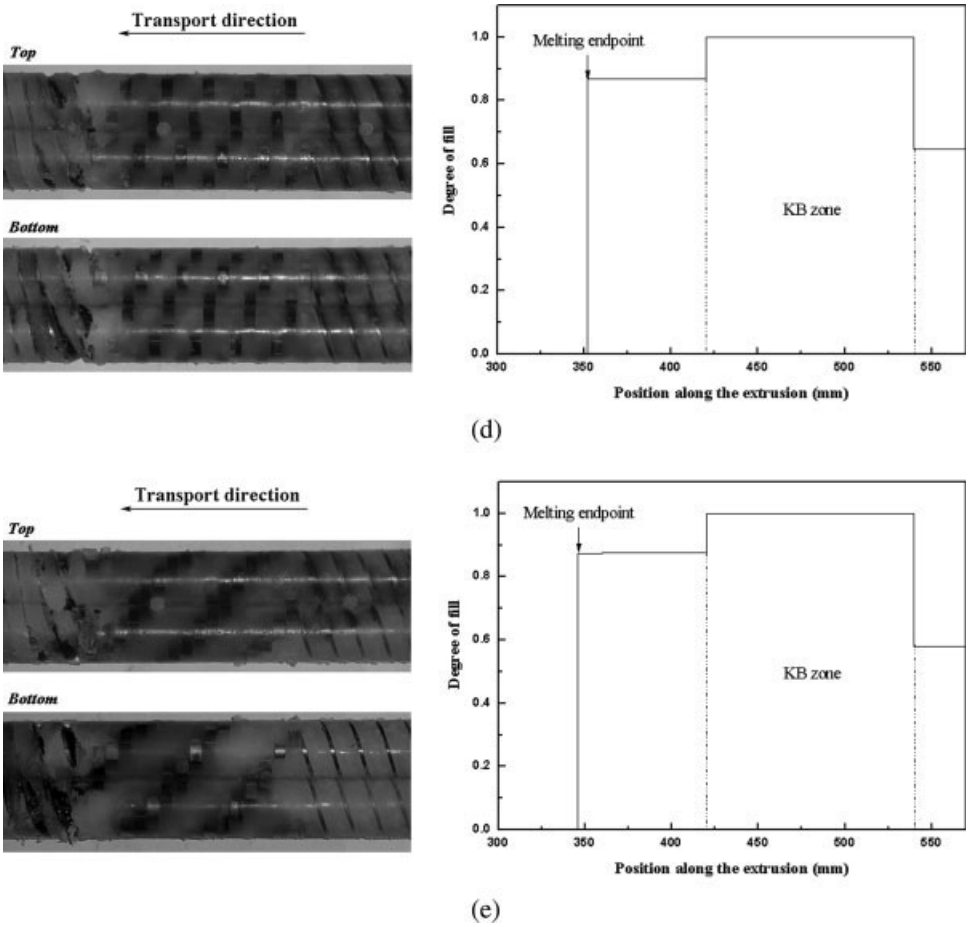

Figure 4 (*Continued from the previous page*)

introduced as well. They could be obtained with the following equations:

$$E(t) = \frac{c(t)}{\sum_1^\infty c(t) \cdot \Delta t} \tag{2}$$

$$\bar{t} = \frac{\sum_1^\infty t \cdot c(t) \cdot \Delta t}{\sum_1^\infty c(t) \cdot \Delta t} = \sum_1^\infty t \cdot E(t) \cdot \Delta t \tag{3}$$

$$\sigma^2 = \frac{\sum_1^\infty (t - \bar{t})^2 \cdot c(t) \cdot \Delta t}{\sum_1^\infty c(t) \cdot \Delta t} = \sum_1^\infty (t - \bar{t})^2 \cdot E(t) \cdot \Delta t \tag{4}$$

where $c(t)$ is the tracer concentration at the extruder outlet.

Because in reactive extrusion the reactant system of LDPE and MA is an immiscible liquid–liquid system, in the fourth group of extrusion experiments, an ABS/PC blend as an immiscible system was introduced to evaluate the mixing performance of each screw configuration. The ABS/PC blend extrudate was collected and then cryogenically fractured along the surface transverse to the extrusion direction. After the fractured samples were coated with gold, they were examined with a Hitachi S-4700 field emission scanning electron microscope (Tokyo, Japan) to check the size of the dispersed phase, that is, PC. The scanning electron microscopy (SEM) pictures were quantitatively analyzed by the counting of the size of the dispersed phase from different fields of the specimen. The average diameter ($\overline{D}$) was calculated from a minimum of 1000 particles as follows:

$$\overline{D} = \frac{\sum N_i D_i}{\sum N_i} \tag{5}$$

where N_i is the number of domains with diameter D_i.

RESULTS AND DISCUSSION

GD

Fourier transform infrared (FTIR) spectra of the grafted products were obtained with a Nicolet 210 FTIR spectrophotometer (Madison, Wisconsin). Figure 3 shows the difference in the FTIR spectra between virgin and grafted LDPE. At 1790 cm^{-1},

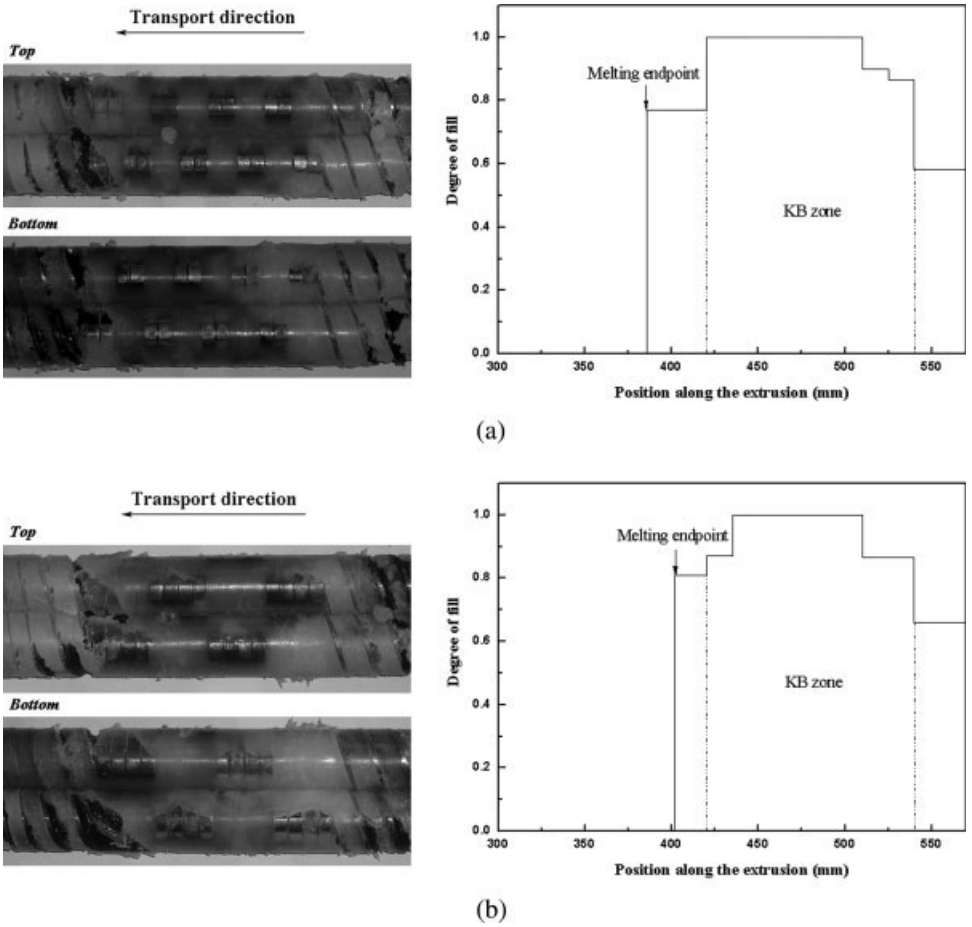

Figure 5 Melting endpoint and degree of fill around the kneading blocks for the screw configurations with wider discs: (a) KB90-2 and (b) KB90-4.

there is a clear signal in the grafted product, but it is absent in the virgin materials. This is ascribed to the stretching of C=O bonds from ester groups of the MA molecules attached to LDPE.

The GD values of all samples collected from various screw configurations are summarized in Table III. For each sample, three to five titrations were performed.[19] It was found that the staggering angle of the kneading blocks has some effects on the GD. The ranking of the GD in decreasing order of the kneading blocks with different staggering angles is 120, 150, 90, 30, and 60° at a disc width of 7.5 mm. On the other hand, for the kneading blocks with different disc widths, designated as screw configurations KB90, KB90-2, and KB90-4, the GD in each sampling point decreases with increasing disc width.

Degree of fill

The melting endpoint is defined as the location in which the solid polymer pellets are melted completely. That is, no solid residues remain. The degree of fill represents the fraction of polymers inside the screw channel. It is less than 1 when the screw channel is partially filled, and a degree of fill of 1 stands for a fully filled channel. Figures 4 and 5 and Table IV summarize the locations of the melting endpoint and the degree of fill in the kneading blocks within different screw configurations.

Generally, the value of the GD along the screw channel depends on both the flow pattern and the mixing intensity of the melt at the upstream flow domain. At sampling point I, the upstream is partially filled for each screw configuration, and the degrees

TABLE IV
Melting Endpoint and Filling Information Corresponding to Figures 4 and 5

Screw code	Melting endpoint (mm)	Degree of fill in the upstream of the KB zone	Fully filled length in the KB zone (mm)
KB30	384	0.424	0
KB60	390	0.754	0
KB90	377	0.882	105
KB120	352	0.868	120
KB150	346	0.874	120
KB90-2	386	0.770	90
KB90-4	402	0.810	75

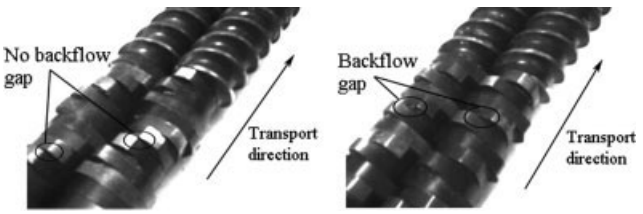

Figure 6 Backflow gap between two adjacent blocks: KB30 (left) and KB60 (right).

of fill at this location are close to each other for various screw configurations, except KB30, in which the degree of fill is lowest. Because little reaction takes place before the material is melted completely,[4] the distance between the melting endpoint and the sampling location determines the GD. The more the melting endpoint moves upstream, the earlier the reaction begins, and the longer the reaction time is. In other words, the GD at sampling point I increases with increasing distance between the melting endpoint and the sampling position. This is fully supported by the data given in Tables III and IV for the processing with various screw configurations, except KB150. However, the reasons for these exceptions are not well understood yet.

On the other hand, the GD at sampling point II is affected by the GD at sampling point I and the flow patterns of the polymer melt in the KB zone. To investigate the roles of the kneading blocks, the increments of the GDs between these two sampling points were calculated, and they are listed in the last column of Table III. The effects of the screw configuration in the KB zone upon reaction are interpreted with three factors: the degree of fill, RTD, and mixing efficiency. Experimental groups ExII, ExIII, and ExIV were designed to explore these factors, respectively.

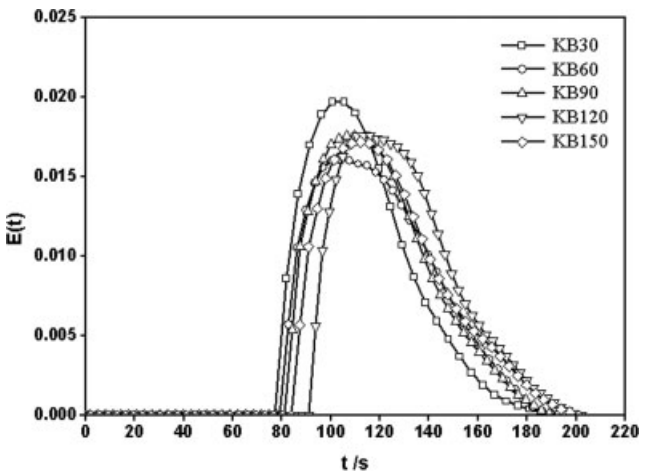

Figure 7 $E(t)$ curves for the screw configurations with various staggering angles.

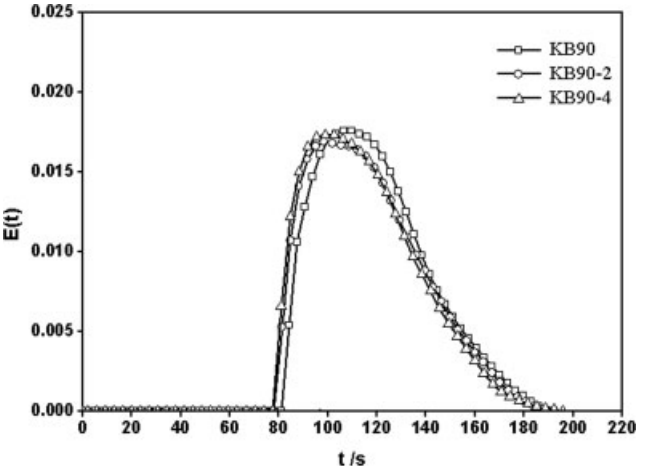

Figure 8 $E(t)$ curves for the screw configurations with wider discs.

As shown by the results of ExII, the flow domains of screw configurations KB30 and KB60 are partially filled along the KB zone. Moreover, it seems that the degree of fill in KB30 is much less than that in KB60. These phenomena can be explained by the forward-conveying capacity of KB30 and KB60. For KB30, there is no backflow gap between two adjacent kneading discs, as shown in Figure 6; this kneading block acts similarly to a conveying screw element with large pitch. There are backflow gaps between any two adjacent kneading discs in KB60, which decrease its forward-conveying ability. For the screw configurations other than KB30 and KB60, the increments in the GDs between sampling points I and II seem in accordance with the fully filled length in the KB zone. In addition, the KB zones of KB120 and KB150 are completely filled. The roles of these kneading blocks in reactive extrusion were further investigated with the following two experimental groups, the RTD and the mixing performance.

RTD

Figures 7 and 8 summarize the results of $E(t)$ for different screw configurations. The values of $\bar{t}$ and σ^2 are also given in Table V. Both $\bar{t}$ and σ^2 from screw configuration KB30 are smaller than those from the others,

TABLE V
Values of $\bar{t}$ and σ^2 for the Screw Configurations

Screw code	$\bar{t}$ (s)	σ^2 (s^2)
KB30	113	417
KB60	118	514
KB90	119	471
KB120	129	475
KB150	124	536
KB90-2	116	488
KB90-4	115	476

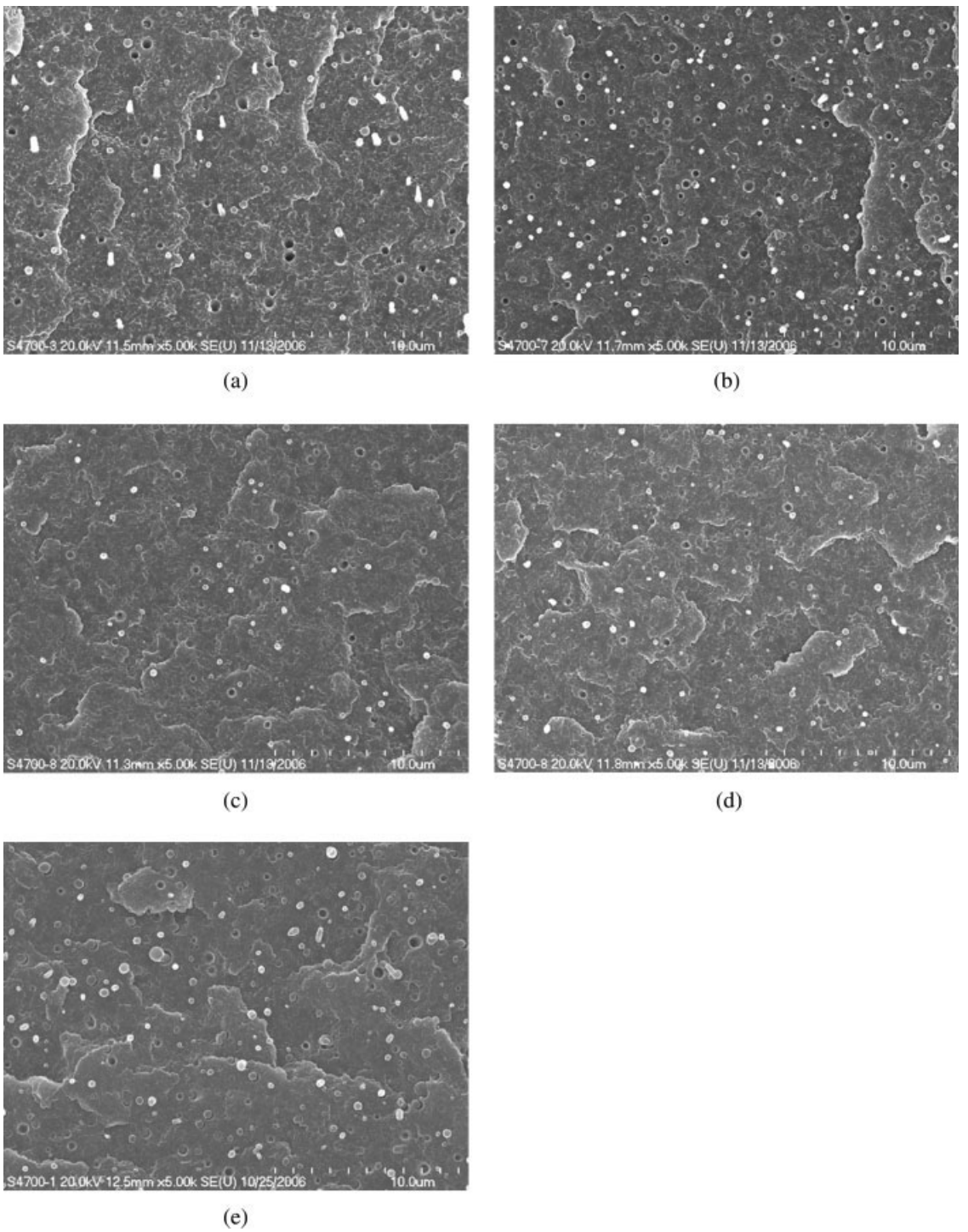

Figure 9 SEM photographs of ABS/PC for the screw configurations with various staggering angles: (a) KB30, (b) KB60, (c) KB90, (d) KB120, and (e) KB150.

and this is mainly due to the lower degree of fill and better forward-conveying ability for KB30. $\bar{t}$ increases with increasing staggering angle of the kneading blocks, except for KB150, but decreases with increasing disc width. However, σ^2 does not have such a relationship with the structure of the kneading blocks.

As shown in Table III, the GDs of the extrudates at the die exit increase when $\bar{t}$ is increased. This can be explained by the fact that increasing $\bar{t}$ enhances the degree of reaction. However, this trend is not applicable for screws KB30, KB90-2, and KB90-4. $\bar{t}$ in KB30 is less than those in KB90-2 and KB90-4, but the GD at the die exit from the former is higher than those from the latter. Moreover, the GD of the extrudate is not proportional to $\bar{t}$ because the reaction depends not only on the reaction time but also on

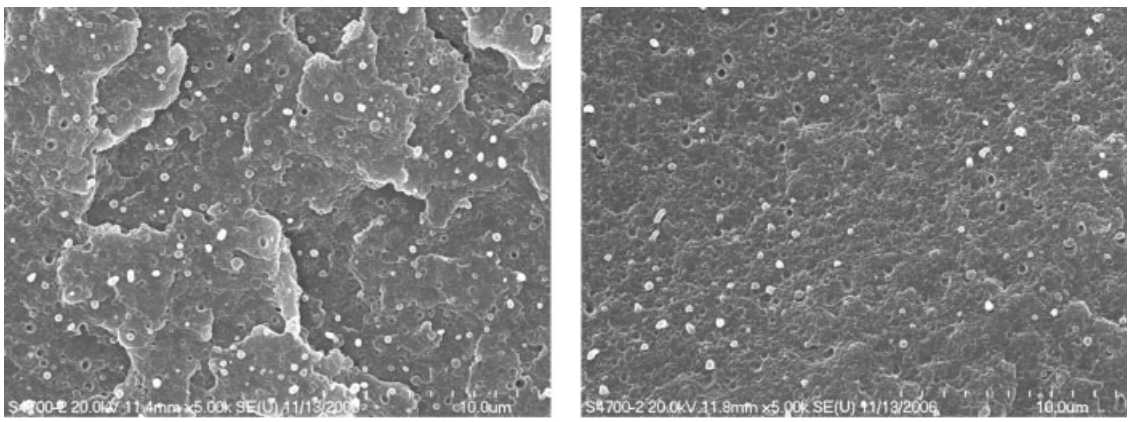

Figure 10 SEM photographs of ABS/PC for the screw configurations with wider discs: (a) KB90-2 and (b) KB90-4.

the temperature profile and homogeneity between the reactants.

Mixing performance of the screw

The morphologies of ABS/PC blends prepared with various screw configurations are shown in Figures 9 and 10 at the same magnification. $\overline{D}$ of the dispersed domain was calculated from micrographs in Figures 9 and 10 on the basis of eq. (5) and is depicted in Figure 11.

As shown in Figures 9 and 10, the phase structure of the blend is inhomogeneous, having dispersed domains as the minor phase in the matrix; this indicates immiscible behavior. The ranking of $\overline{D}$ in Figure 11 in decreasing order for the various screw configurations is KB90-4, KB90-2, KB60, KB30, KB150, KB90, and KB120, which almost agrees with the ranking of the GD of the extrudate in increasing order for the aforementioned screws. This is reasonable because the smaller the size is of MA dispersed in the reactive system; the larger the contacting interface is between MA and LDPE. This would lead to a fast increase in the GD.

Although wide kneading discs provide intense shearing to the polymer melt across their surface, the wider discs mean a lower kneading block number at a fixed length of the KB zone, and this results in less longitudinal mixing. Consequently, narrower discs present better dispersive mixing. For the kneading discs with various staggering angles, reverse-conveying ones present better mixing properties than the forward ones.

CONCLUSIONS

The kneading block configurations have some effects on the grafting reaction progression of LDPE-*g*-MA along the screw in twin-screw extruders. For the kneading blocks with various staggering angles, the ranking of the angles corresponding to the GDs in decreasing order is 120, 150, 90, 30, and 60°. The GDs decrease with increasing disc width.

The location of the melting endpoint determines the position at which the reaction begins. The more the melting endpoint moves upstream, the earlier the reaction begins, and the longer the reaction time is. On the other hand, with increasing staggering angle and decreasing disc width, the degree of fill in the KB zone rises, except for the screw with KB120 and KB150, in which the flow domain is completely filled. According to the experimental results from ExI and ExII, the location of the melting endpoint almost corresponds to the GD at sampling point I, except for screw configurations KB120 and KB150. The fully filled length is one of the important factors for the increase in the GDs in the KB zone.

The RTD plays a significant role in grafting reactive extrusion. In particular, $\bar{t}$ has a direct effect on the reactive time for the reactants in the extruder. However, according to ExI and ExIII, $\bar{t}$ for KB30 is

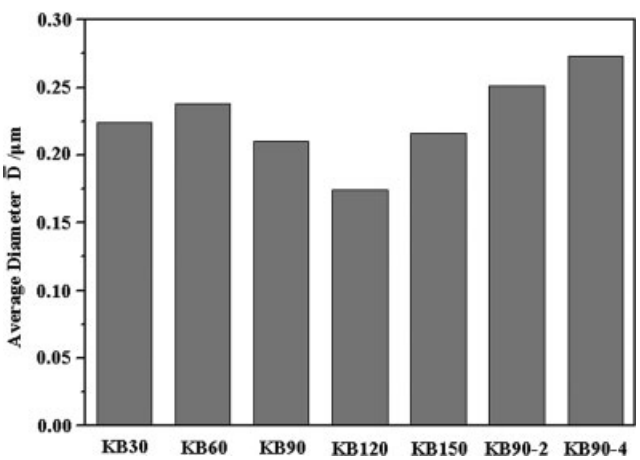

Figure 11 $\overline{D}$ of the dispersed phase in the ABS/PC blend for the screw configurations.

shorter than that for KB90-2 and KB90-4, but the GD for KB30 is higher. In addition, the GD of the extrudate is not proportional to $\bar{t}$ for each screw configuration, and this indicates that the RTD is not the only factor in determining the reactive progress in the reactive extrusion.

The experimental results from the mixing studies of ABS/PC indicate that the GD is related to the mixing capacity of the screw configurations. The screw configuration with better mixing ability could lead to a higher GD in the extrudate. Although the mixing property of the screw is related to the degree of fill and the RTD, the effect of the kneading blocks on the mixing performance cannot be neglected. Consequently, the kneading blocks, such as a reverse-conveying kneading block with a narrow disc, have a high degree of fill and good mixing performance during the extrusion and result in a fast increase in the GD.

References

1. Ganzeveld, K. J.; Janssen, L. P. B. M. Polym Eng Sci 1992, 32, 467.
2. Heinen, W.; Rosenmöller, C. H.; Wenzel, C. B.; de Groot, H. J. M.; Lugtenburg, J.; van Duin, M. Macromolecules 1996, 29, 1151.
3. Machado, A. V.; Covas, J. A.; van Duin, M. Polymer 2001, 42, 3649.
4. Rosales, C.; Márquez, L.; Perera, R.; Rojas, H. Eur Polym J 2003, 39, 1899.
5. Machado, A. V.; van Duin, M.; Covas, J. J Polym Sci Part A: Polym Chem 2000, 38, 3919.
6. Greco, R.; Musto, P.; Riva, F.; Maglio, G. J Appl Polym Sci 1989, 37, 789.
7. Jois, Y. H. R.; Bronk, J. M. Polymer 1996, 37, 4345.
8. Roberts, D. H.; Constable, R. C.; Thiruvengada, S. Polym Eng Sci 1997, 37, 1421.
9. Rosales, C.; Perera, R.; Ichazo, M.; Gonzalez, J.; Rojas, H.; Sánchez, A.; Barrios, A. J Appl Polym Sci 1998, 70, 161.
10. van Duin, M.; Machado, A. V.; Covas, J. Macromol Symp 2001, 170, 29.
11. Samay, G.; Nagy, T.; White, J. L. J Appl Polym Sci 1995, 56, 1423.
12. Nield, S. A.; Budman, H. M.; Tzoganakis, C. Contr Eng Pract 2000, 8, 911.
13. Machado, A. V.; Covas, J. A.; van Duin, M. Adv Polym Technol 2004, 23, 196.
14. Razavi Aghjeh, M. K.; Nazockdast, H.; Assempour, H. J Appl Polym Sci 2006, 99, 141.
15. Shi, Q.; Zhu, L. C.; Cai, C. L.; Yin, J. H.; Costa, G. J Appl Polym Sci 2006, 101, 4301.
16. Pesetskii, S. S.; Jurkowski, B.; Krivoguz, Y. M.; Tomczyk, T.; Makarenko, O. A. J Appl Polym Sci 2006, 102, 5095.
17. Lee, S. Y.; McCarthy, K. L. J Food Eng 1996, 19, 153.
18. Kumar, A.; Ganjyal, G. M.; Jones, D. D.; Hanna, M. A. J Food Eng 2006, 75, 237.
19. Sclavons, M.; Franquinet, P.; Carlier, V.; Verfaillie, G.; Fallais, I.; Legras, R.; Laurent, M.; Thyrion, F. C. Polymer 2000, 41, 1989.